Responsivity enhancement of mid-infrared PbSe detectors using CaF_2 nano-structured antireflective coatings

Binbin Weng,[1,a),b)] Jijun Qiu,[1,b)] Zijian Yuan,[1] Preston R. Larson,[2] Gregory W. Strout,[2] and Zhisheng Shi[1,3,a)]
[1]*School of Electrical and Computer Engineering, University of Oklahoma, Norman, Oklahoma 73019, USA*
[2]*Samuel Roberts Noble Electron Microscopy Laboratory, University of Oklahoma, Norman, Oklahoma 73019, USA*
[3]*Nanolight, Inc., Norman, Oklahoma 73069, USA*

(Received 27 November 2013; accepted 19 December 2013; published online 14 January 2014)

The CaF_2 nano-structures grown by thermal vapor deposition are presented. Significant responsivity improvement (>200%) of mid-infrared PbSe detectors incorporating a 200 nm nano-structured CaF_2 coating was observed. The detector provides a detectivity of 4.2×10^{10} $cm \cdot Hz^{1/2}/W$ at 3.8 μm, which outperforms all the reported un-cooled PbSe detectors. Structural investigations show that the coating is constructed by tapered-shape nanostructures, which creates a gradient refractive-index profile. Analogy to moth-eye antireflective mechanism, the gradient refractive-index nanostructures play the major roles for this antireflection effect. Some other possible mechanisms that help enhance the device performance are also discussed in the work. [http://dx.doi.org/10.1063/1.4861186]

Fresnel reflection due to refractive index mismatch at the interface of dielectric media can significantly deteriorate the performance of many optoelectronic applications, including sensor systems, solid-sate lighting, and energy conversion processes in solar cells. The accelerating demand of such optoelectronic devices extensively stimulates the need in optical engineering research to realize antireflective coatings that maximize light collection efficiency.[1] Conventionally, thin-film antireflective coatings exhibit suppressed reflectivity based on their light destructive interference principle.[2] However, this technique can only work in a limited wavelength range at narrow incidence angles. In addition, due to the refractive index restriction in these antireflective coatings, the availability of suitable coating materials is also very limited.

Originally inspired by the excellent antireflective capability of moth eyes in nature,[3,4] the studies on biomimetic sub-wavelength nanostructured antireflective coatings have been developing quickly.[5] The basic idea is that the nanostructured coating-materials are capable of creating a gradient refractive index profile due to their tapered morphology, and consequently forms their unique broad wavelength antireflection property. In recent years, various nanofabrication techniques[6–11] and new antireflective materials[12–16] have emerged rapidly. Nevertheless, reported works to develop sub-wavelength nanostructured antireflective coatings mainly focus on the antireflective enhancement in the visible and near-IR wavelength ranges.[14,17,23] Similar efforts made in the mid-infrared range are quite few. Lack of a suitable nanostructured coating materials, which have sufficient low light absorption in this wavelength range, could be one of the major reasons. Therefore, in this work, we report on the antireflective coating using calcium fluoride (CaF_2) nano-arrays grown by thermal vapor deposition method under near-room temperature growth conditions. CaF_2 is well known as a window material covering a broad spectrum range from mid-infrared to ultraviolet radiation since it is optically transparent from 0.13 μm to 12 μm.[18–20] This broadband high transmission property is an important advantage in developing antireflective coatings. On the other hand, CaF_2 has very good insulating properties, which makes this material a promising candidate for surface protection and passivation in microelectronics and optoelectronics.[21,22] Therefore, developing a reliable technique to fabricate CaF_2 sub-wavelength nanostructured antireflective coatings could be able to elevate the performance of various optoelectronic devices in mid-infrared wavelength range. In this report, we used room-temperature photoconductive PbSe detectors as an active platform to demonstrate the unique antireflective capabilities of the CaF_2 nanostructured coatings in the mid-IR range.

Figures 1(a) and 1(b) present the top and cross-sectional images of 100 nm thick CaF_2 nanostructure arrays characterized by a ***Zeiss Neon-40 EsB*** high resolution field-emission scanning electron microscope (FESEM). The CaF_2 film was prepared by physical vapor deposition method using a customized thermal evaporation equipment. During the deposition, the background vacuum pressure was kept below 5×10^{-7} Pa while the substrate was spinning at 20 rpm speed to ensure film uniformity. The CaF_2 source heating temperature was controlled at 1350 °C to ensure a stable growth rate. Last but not least, in order to protect the mid-infrared detectors from damaging in a high temperature ambient, the substrate growth temperature was kept at 80 °C. This low temperature constrains the lateral movement of the deposited CaF_2 molecules on the sample surface, which ensures the nanostructures growth and also suppress the large polycrystalline congregations. The images in Figure 1 clearly reveal that the tip of the rods is faceted, and the nanostructure has a roof-tilted shape, which implies the single crystalline nature of the CaF_2.

In addition to the SEM information, the crystalline property is further verified by high resolution transmission electron

a)Electronic addresses: binbinweng@ou.edu and shi@ou.edu
b)B. Weng and J. Qiu contributed equally to this work.

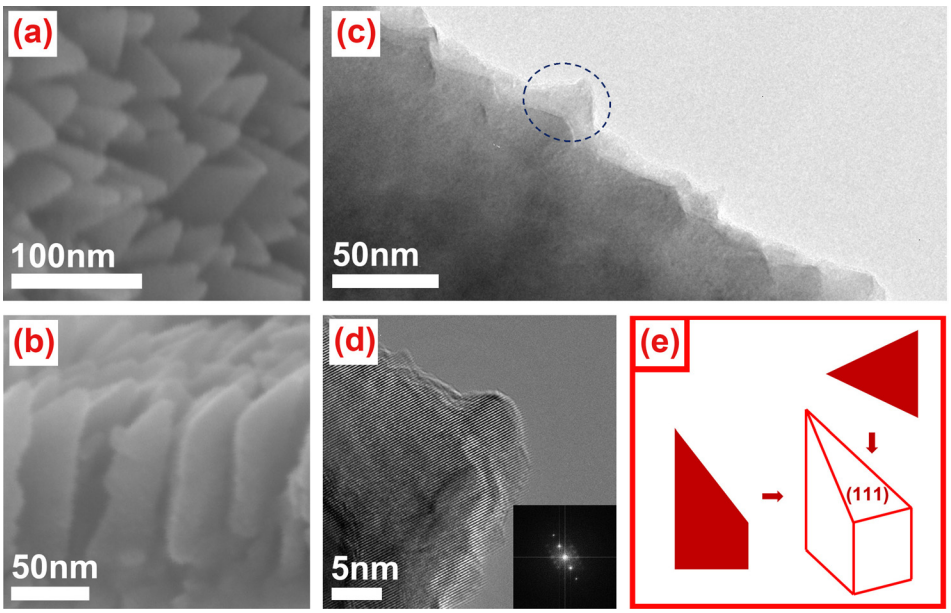

FIG. 1. Characterization of the morphology and microscopic structure of the CaF_2 nanostructures: (a) Top & (b) Cross-sectional high-resolution FESEM images of CaF_2 nanostructure arrays; (c) the tip of the CaF_2 nanostructure arrays shown by high-resolution transmission electron microscopy (HRTEM); (d) HRTEM image of a single CaF_2 nanostructure pyramidlike tip; in-set in (d) shows an FFT from the image (d); (e) schematic model of a single piece CaF_2 nano-structure. (Note: image (d) shows clear atomic plane alignment of CaF_2 material.)

microscopy (TEM). Figures 1(c) and 1(d) present pictures taken by a high resolution ***JEOL JSM 2010-F*** TEM. Figure 1(d) is the magnified image from the circle-marked area in Figure 1(c). Because of its high resolution, Figure 1(d) demonstrates the clear crystallographic structure of the CaF_2 nanostructures at the atomic scale, which offers additional evidence of the single crystalline property of the CaF_2. This conclusion can also be supported by the fast Fourier transformation image shown in the inset in Figure 1(d). It is well known that CaF_2 is a cubic structure having the lowest surface energy planes at {111}.[24] Since the mobility of deposited atoms is fastest on the planes with the lowest surface energy, deposited atoms will spread primarily on these planes to dominate the growth. Therefore, the faceted surface on the tip of each CaF_2 nanostructure should be dominated by a (111) crystallographic face as represented in Figure 1(e). It is well known that nanostructured coating-materials with tapered shapes are capable of creating a gradient refractive index profile, and consequently achieve antireflection in a broad-wavelength range. Therefore, it is also possible that the CaF_2 nanostructures as described above could possess this unique light-reflection property. For the purpose of exhibiting the antireflective properties of the CaF_2 nano-arrays in the mid-IR region, we used mid-infrared room temperature operated PbSe detectors as a simple but effective platform. The PbSe detectors were prepared using a chemical bath deposition method. The aqueous precursor was prepared by dissolving sodium hydroxide, lead acetate and selenosulfate with a concentration ratio of 12:1:1. The glass substrates were transferred into the precursor at 70 °C for 1.5 h. More details can be found by referring to our previous report.[25] To fabricate the PbSe detectors, 200 nm thick gold thin films were deposited by thermal evaporation over two sides of the $4 \times 2\,mm^2$ post iodine-senisitized PbSe material with a $2 \times 2\,mm^2$ active area.

Figure 2 presents the morphologies of the PbSe polycrystalline structures with and without the CaF_2

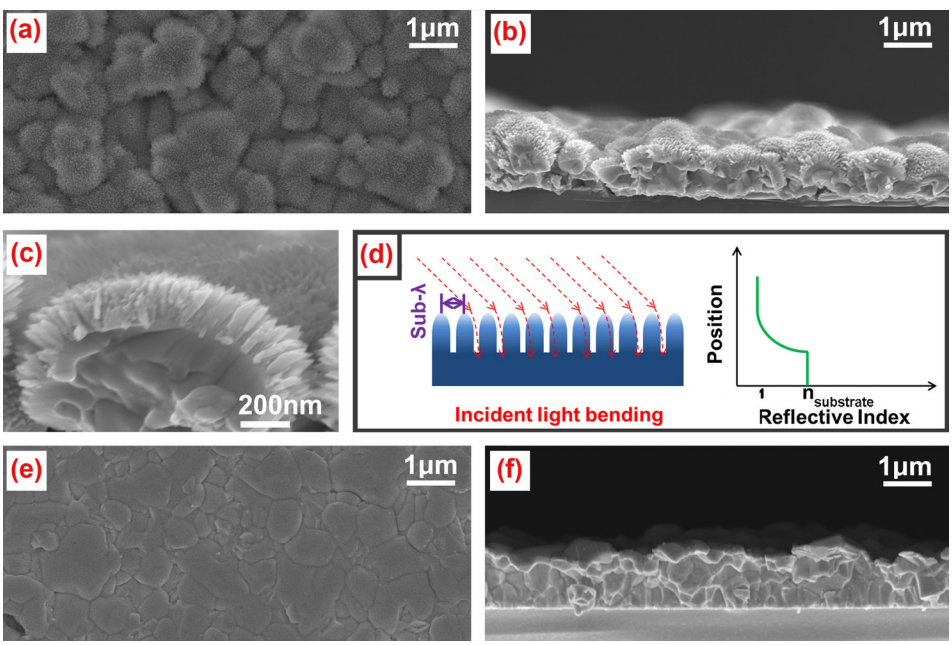

FIG. 2. Morphology of PbSe polycrystalline material and schematics of nanostructure-assisted gradient refractive index principle: (a) top view and (b) cross sectional FE-SEM view of PbSe polycrystalline with CaF_2 nanostructured coating; (c) magnified SEM of one flowerlike CaF_2 nanostructured coated PbSe polycrystalline material; (d) schematics for light bending effect of gradient refractive index nanostructure coating resulted from its sub-wavelength tip-tapered morphology; (e) top and (f) cross sectional views of PbSe polycrystalline with CaF_2 nano-structured coating.

nanostructures arrays coating from top and cross-sectional SEM views. As Figures 2(a) and 2(e) demonstrate, the average size of the PbSe mono-crystalline domain is around ~500 nm, and the surface roughness is also at this sub-micron level. With a 200 nm thick CaF_2 nanostructures coating layer whose single-piece dimension is around 20 nm, each PbSe mono-crystalline domain generates a flowerlike nano-structured layer on its top surface, as shown in Figure 2(b). Although the PbSe crystal size varies, the overall structure demonstrated in Figure 2(c) is quite similar to the moth-eye structure whose antireflection performance is extremely outstanding in nature. In order to highlight the photo-response enhancement by using CaF_2 nano-coatings, conventional PbSe photoconductive detectors were fabricated without the CaF_2 coating as a comparison. Figure 3(a) shows the spectral responsivities for a pristine PbSe detector and the CaF_2 coated detector under the same measurement conditions by using the *Bruker IFS 66/S* FTIR spectrometer. From the figure, it can be observed that there are distinct spectral responses. In the photosensitive spectral range from 2.0 μm up to 5.0 μm, the spectral responsivity of the detector is significantly increased by over 200% in each wavelength in this range by introducing a CaF_2 nanostructures coating layer. To take device noises into consideration, the specific detectivities (D^*) of the photodetectors are presented in Table I by using the definition as shown below

$$\begin{cases} D^* = R \times \dfrac{\sqrt{A \times \Delta f}}{V_n} & (\text{cm} \times \text{Hz}^{1/2}/\text{W}) \\ R = \dfrac{V_s}{P_i} & (\text{V/W}) \end{cases},$$

where R is the detector responsivity, V_s and V_n are the measured detector output signal and noise voltages, A is the device detection area, Δf is the noise bandwidth, and P_i is the incident radiant power. For these detectivities measurement, a *Thorlabs* mechanical chopper was used to modulate a collimated 500 K blackbody from *Infrared System Development Corp.* in order to provide a frequency-modulated heat source, and the detectors were biased at 100 V using an Agilent E3612A voltage source with a load resistor matched to the sensor resistance. Both signal and noise voltages were collected by a *Stanford Research System SR830* lock-in amplifier after a self-made preamplifier. Under 750 Hz chopping frequency modulation, the detector with the CaF_2 coating provides a peak detectivity of 4.2×10^{10} cm · $\text{Hz}^{1/2}$/W at 3.8 μm at room temperature, which outperformed all the existing un-cooled mid-infrared PbSe detectors. Note that except for the difference in the final CaF_2 coating step, the two detectors were fabricated using the same process flow in the same run, and the CaF_2 deposition was carried out by maintaining the growth temperature at 80 °C to ensure no change in the properties of the PbSe detector itself. In other words, the light detection improvement of the detectors is due to the CaF_2 nano-structures coating.

To investigate the functionalities of the CaF_2 coating layer, the total reflection spectra and photoluminescence (PL) with a Nd:YAG pulse pumping laser were both measured by the *Bruker IFS 66/S* FTIR spectrometer. The results are as shown in Figures 3(b) and 3(c).

In Figure 3(b), it is clear that the CaF_2 nano-structured coating layer reduces the reflection over a wide range of wavelengths in the mid-infrared PbSe photosensitive region effectively. Compared with the pristine detector, the reflectance of the detector with CaF_2 nano-structured coating is decreased from 21% to 12% at 3.8 μm, which is the peak response position as shown in Figure 3(a). Since the 200 nm coating thickness is far less than quarter-wave film thickness ~670 nm ($\lambda/4n_{CaF2}$), the thin film destructive interference mechanism is not applicable to explain these light coupling phenomenon between PbSe films and the ambient air. As mentioned, the CaF_2 nano-arrays coated on the PbSe polycrystalline structure is similar to the moth-eye structure found in nature. Based on the moth-eye's antireflective mechanism, primarily due to the tapered shape of the CaF_2

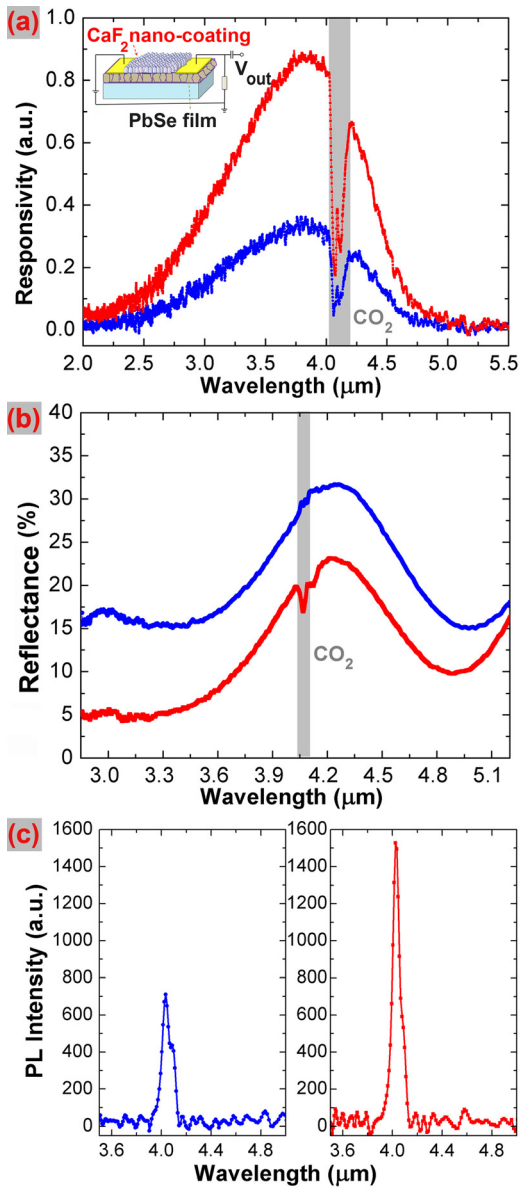

FIG. 3. Influence of the CaF_2 nanostructured antireflective coatings on the PbSe detector and its optical properties: (a) spectral response curves of the sensor (inset is a schematic of PbSe detector with the CaF_2 coating); (b) reflection spectrum and (c) photoluminescence spectrum of the PbSe thin films on sensor. (Red-colored data: PbSe with the CaF_2 coating; Blue-colored data: PbSe without the CaF_2 coating.)

TABLE I. The Performance characterizations of the PbSe detectors. (Note: active area: 2×2 mm^2, bias voltage: 25 V/mm, and chopping frequency: 750 Hz.)

Samples#	CaF_2 coating	Noise voltage (μV)	Responsivity at λ_p (V/W)	D* (λ_p, 500 K, 1 Hz) (cm · Hz$^{1/2}$/W)
1	yes	0.25	5.25×10^4	4.2×10^{10}
2	no	0.25	2.50×10^4	2.0×10^{10}

nano-structure tips, the filling factor (the area of CaF_2 to the total surface area) of the CaF_2 nano-arrays increases with the depth approaching the CaF_2/PbSe interface, which eventually leads to a better effective refractive index transition from the surface of the PbSe detector to the ambient air. Since the CaF_2 nano-structured coating layer has a gradient refractive index profile, and its nano-structure dimension is greatly below the wavelength of incident light,[1] the incident light rays tend to bend progressively giving rise to the broadband antireflection performance, as demonstrated by Figure 2(d).

The pulsed laser pumped PL spectra emitted from the PbSe films of the pristine detector and the CaF_2 coated detector is shown in Figure 3(c). The peak emitting position is at around 4.0 μm for both detectors. And the peak intensity of the PL emission collected from the detector sample with the CaF_2 coating is ~2 times greater than the one collected from the pristine uncoated detector. Since the only difference between these two detectors is with and without the CaF_2 coating, this nano-structured coating layer must have played a vital role in helping light couplings between the PbSe film and the ambient air.

Although the coating layer helps reduce the reflection by ~50%, the total light transmission improvement is only ~9% with the coating. Both the detectivity and PL intensity enhancement are much higher than the transmission improvement. Consequently, the CaF_2 nano-structured coating must have played other roles for such significant enhancement of detectivity and PL intensity. First, the CaF_2 coating could have served as a surface passivation layer, which can effectively prolong the photon generated carrier lifetime, as reported in our previous work.[22] But we did not observe any change in dark current after the CaF_2 coating. Second, the CaF_2 nano-structures could increase incident light lateral scattering and prolong the photon travelling path. Third, due to the surface morphology of the polycrystalline PbSe, the CaF_2 coating grown on top formed curved surfaces as shown in Figure 2(c), which could focus the incident light similar as the convex optical lens does. These and perhaps other possible mechanisms that are responsible for enhancement of detectivity and PL intensity require further investigation in future.

In summary, we proposed a thin nano-structured CaF_2 antireflective coating by using a thermal vapor deposition method. To evaluate its functionalities, we used mid-IR room-temperature operating PbSe detectors as a test bed. The detector with the nano-structured CaF_2 coating exhibited broadband responsivity enhancement of over 200% compared to the uncoated detector, leading to a room temperature peak detectivity of 4.2×10^{10} cm · Hz$^{1/2}$/W at 3.8 μm. This promising result of device performance improvement also provides strong motivation to use such nano-structured CaF_2 coating for other opto-electronic devices development.

We acknowledge financial supports from the DoD AFOSR under Grant No. FA9550-12-1-0451, DoD ARO Grant No. W911NF-07-1-0587, and Oklahoma OCAST program under Grant Nos. AR112-18 and AR132-003.

[1]H. K. Raut, V. A. Ganesh, A. S. Nair, and S. Ramakrishna, Energy Environ. Sci. **4**, 3779–3804 (2011).
[2]G. R. Fowles, *Introduction to Modern Optics*, 2nd ed. (Dover Publications, New York, 1989).
[3]P. B. Clapham and M. C. Hutkey, Nature **244**, 281–282 (1973).
[4]C. G. Bernhard, "Structural and functional adaptation in a visual system," Endeavor **26**, 79–84 (1967).
[5]R. Brunner, O. Sandfuchs, C. Pacholski, C. Morhard, and J. Spatz, Laser Photon. Rev. **6**, 641–659 (2012).
[6]B. Päivänranta, P. Sahoo, C. David, V. Auzelyte, Y. Ekinci, H. H. Solak, E. J. Tocce, C. Liu, K. O. Stuen, and P. F. Nealey, ACS Nano **5**, 1860–1864 (2011).
[7]C. Chang, J. A. Dominguez-Caballero, H. J. Choi, and G. Barbastathis, Opt. Lett. **36**, 2354–2356 (2011).
[8]O. L. Muskens, J. G. Rivas, R. E. Algra, E. P. A. M. Bakkers, and A. Lagendijk, Nano Lett. **8**, 2638–2642 (2008).
[9]N. C. Linn, C.-H. Sun, P. Jiang, and B. Jiang, Appl. Phys. Lett. **91**, 101108 (2007).
[10]S. Chattopadhyay, L.-C. Chen, and K.-H. Chen, Crit. Rev. Solid State Mater. Sci. **31**, 15–53 (2006).
[11]Q. Xu, Z. Liu, Y. Li, Q. Wu, and S. Zhang, Chin. Phys. Lett. **28**, 024209 (2011).
[12]K.-C. Park, H. J. Choi, C.-H. Chang, R. E. Cohen, G. H. McKinley, and G. Barbastathis, ACS Nano **6**, 3789–3799 (2012).
[13]Y.-C. Chao, C.-Y. Chen, C.-A. Lin, Y.-A. Dai, and J.-H. He, J. Mater. Chem. **20**, 8134–8138 (2010).
[14]M.-L. Kuo, D. J. Poxson, Y. S. Kim, F. W. Mont, J. K. Kim, E. F. Schubert, and S.-Y. Lin, Opt. Lett. **33**, 2527–2529 (2008).
[15]J.-Q. Xi, M. F. Schubert, J. K. Kim, E. F. Schubert, M. Chen, S.-Y. Lin, W. Liu, and J. A. Smart, Nature Photon. **1**, 176–179 (2007).
[16]Y.-F. Huang, S. Chattopadhyay, Y.-J. Jen, C.-Y. Peng, T.-A. Liu, Y.-K. Hsu, C.-L. Pan, H.-C. Lo, C.-H. Hsu, Y.-H. Chang, C.-S. Lee, K.-H. Chen, and L.-C. Chen, Nat. Nanotechnol. **2**, 770–774 (2007).
[17]J. K. Kim, S. Chhajed, M. F. Schubert, E. F. Schubert, A. J. Fischer, M. H. Crawford, J. Cho, H. Kim, and C. Sone, Adv. Mater. **20**, 801–804 (2008).
[18]R. S. Retherford, R. Sabia, and V. P. Sokira, Appl. Surf. Sci. **183**, 264–269 (2001).
[19]D. E. McCarthy, Appl. Opt. **2**, 591–595 (1963).
[20]D. C. Harris, *Materials for Infrared Windows and Domes: Properties and Performance* (SPIE-The International Society for Optical Engineering, Bellingham, 1999).
[21]D. M. Hill, H. M. Meyer, J. H. Weaver, and D. L. Nelson, Appl. Phys. Lett. **53**, 1657 (1988).
[22]S. Mukherjee, D. Li, G. Bi, J. Ma, S. Elizondo, A. Gautam, and Z. Shi, Microelectron. Eng. **88**, 314–317 (2011).
[23]D.-S. Tsai, C.-A. Lin, W.-C. Lien, H.-C. Chang, Y.-L. Wang, and J.-H. He, ACS Nano **5**, 7748–7753 (2011).
[24]T.-M. Lu, F. Tang, and G.-C. Wang, Proc. SPIE **7041**, 704107 (2008).
[25]J. Qiu, B. Weng, Z. Yuan, and Z. Shi, J. Appl. Phys. **113**, 103102 (2013).